Phase diagram of magnetic ladders constructed from a composite-spin model

Örs Legeza
Research Institute for Solid State Physics, H-1525 Budapest, P.O. Box 49, Hungary
and Technical University of Budapest, H-1521 Budapest, Hungary

Gábor Fáth*
Institute of Theoretical Physics, University of Lausanne, CH-1015 Lausanne, Switzerland

Jenő Sólyom
Research Institute for Solid State Physics, H-1525 Budapest, P.O. Box 49, Hungary
(Received 15 July 1996)

White's density matrix renormalization group method has been applied to an $S=1/2+1/2$ composite-spin model, which can also be considered as a two-leg ladder model. By appropriate choices of the coupling constants this model allows one not only to study how the gap is opened around the gapless integrable models, but also to interpolate continuously between models with different spin lengths. We have found indications for the existence of several different massive phases. [S0163-1829(97)02301-1]

I. INTRODUCTION

The recent discovery of several families of new materials,[1–3] such as $(VO)_2P_2O_7$, $Sr_{n-1}Cu_nO_{2n-1}$ $(n=2,3,\ldots)$, and $La_{4+4n}Cu_{8+2n}O_{14+8n}$, where the spin chains are coupled in a special way to form ladders, gave a new impetus to the study of the properties of low-dimensional magnetic systems. This field had already been intensively studied both experimentally and theoretically in the last decade due to a large extent to the proposal by Haldane[4] that antiferromagnetic spin chains described by an isotropic Heisenberg model develop a gap in their excitation spectrum for integer spin, while for half-integer spin the spectrum is gapless.

The spin-ladder models, beside their relevance to these materials, are of special interest for theorists[5–15] because by appropriate choice of the couplings they can describe both spin-1/2 and effective spin-1 models, and they are also related to the models proposed to understand the behavior of the so-called high-T_c materials. Experimental studies[16,17] confirm that two-leg ladders behave like integer-spin models and have a finite gap, while materials with three-leg ladders have a gapless magnetic excitation spectrum.

A particular way to construct ladder models is to put a composite spin on every site of a single chain and to couple the individual spins in various ways.[18,19] This model has already been studied numerically using the Lanczos algorithm to calculate the low-lying energy levels. This method could, however, be applied to relatively short chains only, and therefore the conclusions were sometimes contradictory.

Recently White[20] has proposed a procedure, the density matrix renormalization group (DMRG) method, which allows one to calculate the energy of low-lying levels and related physical quantities on much longer chains. This led to great progress in the application of the finite-size scaling method and allowed the investigation of more complex systems in a larger parameter space.

A natural extension of the usual Heisenberg model of spin chains for $S>1/2$ is to include higher-order polynomials of the bilinear exchange term. In the spin-1 case, where biquadratic exchange can be taken into account, generically the spectrum remains massive,[21] but at some special values of the couplings[22,23] the gap might disappear and the model can be studied by Bethe's ansatz. The opening of the gap around these critical integrable points is, however, not quite settled.

The aim of this paper is to extend the earlier calculations on the composite-spin model to longer chains using the DMRG procedure, and to clarify the phase diagram of the corresponding ladder model.

The setup of the paper is as follows. In Sec. II we give a short description of the composite-spin and ladder models and their relationship to the integrable models for appropriate choices of the parameters. The DMRG method and the numerical procedures are discussed in Sec. III. The results of our numerical calculations are presented in Sec. IV. Finally Sec. V contains a brief summary.

II. COMPOSITE-SPIN AND LADDER MODELS

In a composite-spin model the spin S_i at the lattice site i is composed of two or more spin operators $\sigma_{i\alpha}$ $(\alpha=1,2,\ldots)$. In the most general case the model contains on-site and nearest-neighbor interactions among all spin species with different coupling constants. In this paper we will focus on a model where two $s=1/2$ spin species, from which an $S=1$ spin can be constructed, are put on every lattice site.

The model is defined by starting from the most general isotropic spin-1 model, the bilinear-biquadratic model, which usually is written in the form

$$\mathcal{H}=\sum_i \left[\cos\theta(\vec{S}_i\cdot\vec{S}_{i+1})+\sin\theta(\vec{S}_i\cdot\vec{S}_{i+1})^2\right]. \qquad (1)$$

In the composite-spin representation, where $\vec{S}_i$ can be obtained by adding up the two spin-1/2 species denoted by $\vec{\sigma}_i$

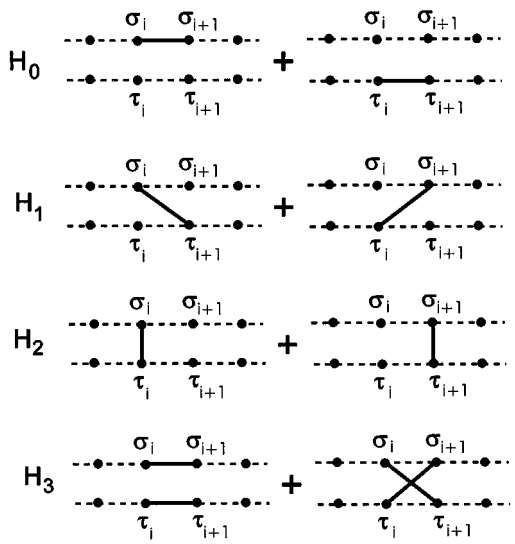

FIG. 1. Schematic plot of the spin couplings in $\mathcal{H}_0$, $\mathcal{H}_1$, $\mathcal{H}_2$, and $\mathcal{H}_3$ between the spins $\vec{\sigma}_i$ and $\vec{\tau}_i$ on the two legs of a ladder.

and $\vec{\tau}_i$, $\vec{S}_i=\vec{\sigma}_i+\vec{\tau}_i$, the Hamiltonian takes the form

$$\mathcal{H}=\left(\cos\theta-\frac{1}{2}\sin\theta\right)(\mathcal{H}_0+\mathcal{H}_1)+2\sin\theta(\mathcal{H}_2+\mathcal{H}_3)+\frac{3(N-1)}{4}\sin\theta, \tag{2}$$

where N is the number of lattice sites in the chain, and

$$\mathcal{H}_0=\sum_i\ [\vec{\sigma}_i\cdot\vec{\sigma}_{i+1}+\vec{\tau}_i\cdot\vec{\tau}_{i+1}], \tag{3a}$$

$$\mathcal{H}_1=\sum_i\ [\vec{\sigma}_i\cdot\vec{\tau}_{i+1}+\vec{\tau}_i\cdot\vec{\sigma}_{i+1}], \tag{3b}$$

$$\mathcal{H}_2=\frac{1}{2}\sum_i\ [\vec{\sigma}_i\cdot\vec{\tau}_i+\vec{\sigma}_{i+1}\cdot\vec{\tau}_{i+1}], \tag{3c}$$

$$\mathcal{H}_3=\sum_i\ [(\vec{\sigma}_i\cdot\vec{\sigma}_{i+1})(\vec{\tau}_i\cdot\vec{\tau}_{i+1})+(\vec{\sigma}_i\cdot\vec{\tau}_{i+1})(\vec{\tau}_i\cdot\vec{\sigma}_{i+1})]. \tag{3d}$$

We will generalize Eq. (2) and consider the model described by the Hamiltonian

$$\mathcal{H}=\lambda_0\mathcal{H}_0+\lambda_1\mathcal{H}_1+\lambda_2\mathcal{H}_2+\lambda_3\mathcal{H}_3, \tag{4}$$

with arbitrary couplings λ_i.

Alternatively, instead of considering $\vec{\sigma}_i$ and $\vec{\tau}_i$ as spins sitting on the same site, we can treat them as sitting on two parallel chains, or on the legs of a ladder, the $\vec{\sigma}_i$ spins on one leg and the $\vec{\tau}_i$ spins on the other. As shown in Fig. 1, $\mathcal{H}_0$ couples spins on the same leg only; the others contain interleg couplings. $\mathcal{H}_2$ is the usual coupling between spins on the same rung, and $\mathcal{H}_1$ couples spins on neighboring rungs of the legs, while $\mathcal{H}_3$ describes four-spin couplings on a plaquette.

Usually the ladder models are constructed to include $\mathcal{H}_0$ and $\mathcal{H}_2$ only. When a strong ferromagnetic coupling is applied across the rungs ($\lambda_2\to-\infty$), the two spins form a triplet and the properties of the $S=1$ Heisenberg chain are recovered.[5,8] In another approach Barnes *et al.*[9] allowed for strong antiferromagnetic interchain couplings and treated $\mathcal{H}_0$ as perturbation. They have shown the existence of a spin gap for any finite interchain coupling.

In the composite-spin model, on the other hand, $\mathcal{H}_1$ is also necessarily included. A special feature of the model is that for arbitrary values of λ_2 and λ_3 the model is invariant under the interchange of λ_0 and λ_1; i.e., the energy levels of the full Hamiltonian satisfy

$$E(\lambda_0,\lambda_1,\lambda_2,\lambda_3)=E(\lambda_1,\lambda_0,\lambda_2,\lambda_3). \tag{5}$$

This can be shown by interchanging the $\vec{\sigma}_i$ and $\vec{\tau}_i$ spins on every second site. This relationship allows one to connect the weak- and strong-coupling limits of the model by a duality transformation. To show this let us denote by ε the energies of the Hamiltonian in which the coupling strength of $\mathcal{H}_0$ is chosen to be unity:

$$E(\lambda_0,\lambda_1,\lambda_2,\lambda_3)=\lambda_0\varepsilon\left(\frac{\lambda_1}{\lambda_0},\frac{\lambda_2}{\lambda_0},\frac{\lambda_3}{\lambda_0}\right). \tag{6}$$

From Eq. (5) it follows that

$$\lambda_0\varepsilon\left(\frac{\lambda_1}{\lambda_0},\frac{\lambda_2}{\lambda_0},\frac{\lambda_3}{\lambda_0}\right)=\lambda_1\varepsilon\left(\frac{\lambda_0}{\lambda_1},\frac{\lambda_2}{\lambda_1},\frac{\lambda_3}{\lambda_1}\right). \tag{7}$$

Introducing the couplings $\tilde{\lambda}_i=\lambda_i/\lambda_0$ ($i=1,2,3$), we get

$$\varepsilon(\tilde{\lambda}_1,\tilde{\lambda}_2,\tilde{\lambda}_3)=\tilde{\lambda}_1\varepsilon\left(\frac{1}{\tilde{\lambda}_1},\frac{\tilde{\lambda}_2}{\tilde{\lambda}_1},\frac{\tilde{\lambda}_3}{\tilde{\lambda}_1}\right). \tag{8}$$

In what follows we will always work with the Hamiltonian in which $\lambda_0=1$ and will drop the tilde over the couplings.

For $\lambda_2=\lambda_3=0$ this relationship reduces to a usual duality relationship, which connects the energies in the $0<\lambda_1\leqslant1$ region to those in $1\leqslant\lambda_1<\infty$,

$$\varepsilon(\lambda_1)=\lambda_1\varepsilon(1/\lambda_1). \tag{9}$$

When $\lambda_1<0$, the above deduced duality relationship connects the lowest-lying levels of one region to the highest-lying levels in the other region. Since in the numerical calculations a few low-lying levels can only be calculated with sufficient precision, a more useful relation can be derived in this case by comparing the energies of $\mathcal{H}$ defined by Eq. (4) with $\lambda_0=1$ to that of $\mathcal{H}'=-\mathcal{H}$. Denoting by $\varepsilon'(\lambda_1,\lambda_2,\lambda_3)$ the energies of this model,

$$\varepsilon'(\lambda_1,\lambda_2,\lambda_3)=-\lambda_1\varepsilon\left(\frac{1}{\lambda_1},\frac{\lambda_2}{\lambda_1},\frac{\lambda_3}{\lambda_1}\right). \tag{10}$$

We used these relations to check the accuracy of the numerical calculations.

According to Eq. (2) the spin-1 model can be reproduced when $\mathcal{H}_0$ and $\mathcal{H}_1$ are taken with equal coupling strength, $\lambda_0=\lambda_1$. When this coupling is antiferromagnetic, it gives rise to a valence-bond configuration[24] of the neighboring spins, which is a characteristic feature of the Haldane phase. When no direct coupling exists between the $\vec{\sigma}_i$ and $\vec{\tau}_i$ spins, nothing ensures *a priori* that these spins appear in the sym-

metric $S=1$ configuration only. When, however, λ_2 and λ_3 are small compared to $\lambda_0=\lambda_1$, the level structure of the true spin-1 model and that of the composite-spin model is such that their low-lying parts coincide, and thus their behavior is similar. Therefore the phase diagram of our ladder model will contain phases characteristic to the bilinear-biquadratic model, but also new phases may appear.

The normalization $\lambda_0=1$ is equivalent to considering the region $-\pi/2<\theta<\pi/2$ only. The bilinear-biquadratic model has a rich phase structure in that region. It has been thoroughly investigated both analytically[21,25] by using, e.g., the mapping to the Wess-Zumino-Witten model, or to the nine-state Potts model and numerically.[26–29] The region $\pi/2<\theta<3\pi/2$ is somewhat less interesting, since the model is ferromagnetic for $\pi/2<\theta<5\pi/4$. Beyond that a new phase might appear, as predicted by Chubukov,[31] although so far its existence has not been confirmed by numerical calculations.[32] This problem is, however, outside the scope of this paper.

$\theta_{\rm TB}=-\pi/4$ corresponds to the Takhtajan-Babujian[22] integrable model with gapless excitation spectrum. This point is the critical point of a second-order Ising-type phase transition with a gap opening linearly around the transition point. In a chain with periodic boundary condition (PBC) the ground state is doubly degenerate for $\theta<-\pi/4$, producing a dimerized phase, while for $-\pi/4<\theta<\pi/4$ the Haldane phase appears with a nondegenerate singlet ground state. This latter region includes the isotropic Heisenberg point at $\theta=0$ and the exact nearest-neighbor valence-bond state[24] (VBS) at $\theta_{\rm VBS}=\arctan(1/3)$.

$\theta_{\rm LS}=\pi/4$ is another integrable point related to the Lai-Sutherland[23] model, where the gap vanishes again. For $\theta>\pi/4$ a trimerized massless phase appears.[28–30] In the composite-spin representation these points lie on the line $\lambda_1=1$, at $\lambda_2=\lambda_3=-4/3$ for the Takhtajan-Babujian, at $\lambda_2=\lambda_3=0$ for the Heisenberg, at $\lambda_2=\lambda_3=4/5$ for the VBS, and at $\lambda_2=\lambda_3=4$ for the Lai-Sutherland points.

Furthermore, the composite-spin Hamiltonian can be transformed into a nonlinear σ model and the results obtained in field theory can be related to our model. At $\lambda_1=\lambda_2=\lambda_3=0$, when the model reduces to two decoupled spin-1/2 chains, the field theory possesses a gapless excitation spectrum because the topological angle is an odd multiple of π. According to the field-theoretical calculations[21] the perturbations around this multicritical point are generically relevant and give rise to the opening of an energy gap, except for special points or lines. The Takhtajan-Babujian and Lai-Sutherland models belong to such exceptions. Consequently, it is expected that by varying the λ_i parameters the gap vanishes only at the critical points and on the phase boundaries between the various phases.

In order to simplify the calculations, first we study the effect of $\mathcal{H}_1$, $\mathcal{H}_2$, and $\mathcal{H}_3$ separately for fixed $\lambda_0=1$. Then the calculation will be extended to a two-parameter plane (λ_1,λ_2) by choosing $\lambda_3=\lambda_2$. In order to determine the phase diagram we examine the low-lying energy levels along different paths connecting those points in parameter space where the model is integrable. The ground-state configurations will also be investigated by calculating the local energy of a bond, the two-point correlation functions, and a short-range order parameter.

III. NUMERICAL PROCEDURES

We have performed numerical calculations by applying the DMRG method[20] on the model defined by the Hamiltonian in Eqs. (3) and (4). This is a real-space renormalization method where the lattice is built up gradually to the desired length, systematically truncating in the meantime the Hilbert space by keeping only the most probable states.

Since the DMRG method works best for systems with free ends, we will consider our composite-spin model with an open boundary condition (OBC). An unfavorable consequence of the OBC for the spin-1 model and consequently for the ladder models as well is that the degeneracies in the spectrum may be different from that obtained for a closed ring. In the nearest-neighbor valence-bond configuration, e.g., free $s=1/2$ spins remain at the ends of the chain, giving rise to a fourfold-degenerate ground state. In the dimerized state, on the other hand, the twofold degeneracy of the ground state is lifted if the number of sites is an even number. This makes the analysis of the spectrum more difficult.

Moreover, in the case of the OBC the total momentum is not a good quantum number. Therefore, only the total spin S_T and its projection to the quantization axis, S_T^z, can be used to classify the energy levels. Since in the isotropic case the SU(2) symmetry is satisfied, the spectrum was analyzed by calculating a few low-lying levels of the different S_T^z sectors. S_T was determined from the degeneracy of the levels.

Because our aim is to determine the overall behavior of the energy spectrum and to identify from it the possible phases, in most of the calculations we have used the less accurate version of DMRG, the so-called *infinite-lattice method*. In this algorithm the lattice is built up by adding two lattice sites in each step. The results obtained for chains with $N=4,8,16,32,48,64$ sites were used in a finite-size scaling procedure to extrapolate to an infinite lattice. On the other hand, close to the critical points and in those regions where the gap is small, the *finite-lattice method* was applied with two or three iteration cycles to determine the energies more precisely.

In some cases, before doing the DMRG calculation on long chains, the energy spectrum was determined by exact diagonalization on short chains with $N=4,6,8$. This gave an idea of the sequence of the levels for different choices of the couplings and allowed us to determine which states have to be targeted in the DMRG procedure.

Considering our limited computational resources, we had to restrict rather drastically the number of states, M, to be kept in the DMRG algorithm. A number that can be used to characterize the numerical accuracy of the DMRG method is the discarded density-matrix weight (truncation error).[20] In the calculation of the ground-state energy for ladders with $N=2\times64$ ($N=2\times32$) sites it was largest close to the critical points with values of the order 10^{-5}–10^{-6} (10^{-7}–10^{-8}), while around the VBS point, where the gap is large, it was as small as 10^{-10}–10^{-11} (10^{-11}–10^{-12}). For the excited states the truncation error was worse by one order of magnitude.

The real error in the DMRG procedure can, however, be much worse.[33] It was estimated by comparing the energies obtained for the ladder model using the DMRG procedure to those of the spin-1 bilinear-biquadratic model or the spin-1/2

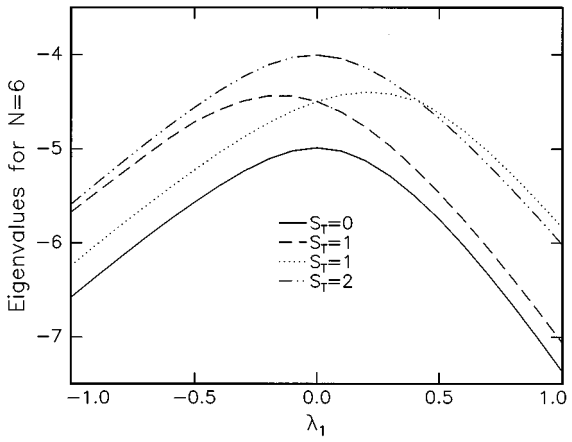

FIG. 2. Low-lying energy spectrum of the Hamiltonian as a function of λ_1 ($\lambda_2=\lambda_3=0$) for chain length $N=6$.

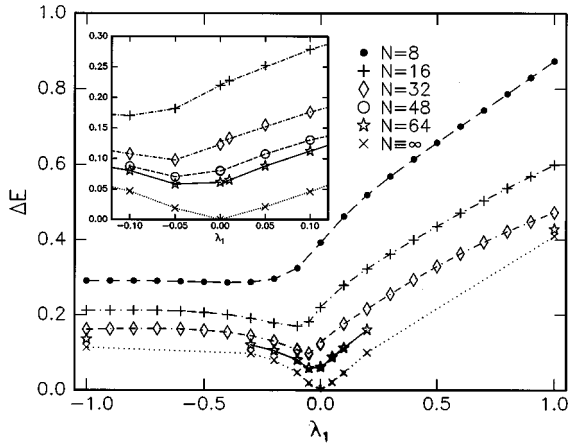

FIG. 3. The energy difference between the low-lying levels of our model as a function of λ_1 at $\lambda_2=\lambda_3=0$ for chain lengths $8\leqslant N\leqslant 64$. For $\lambda_1>0$ ΔE_{21}, while for $\lambda_1<0$ ΔE_{10} is shown. The dotted line is the gap extrapolated for $N\to\infty$. The inset shows the behavior for small values of λ_1.

chain, where much better accuracy can be achieved. For chains with $N=2\times 32$ sites an agreement up to three or four decimal places has been achieved after the second iteration cycle of the finite-lattice method, if M was chosen to be $M=64$, while for chains with $N=2\times 64$ sites the same accuracy required us to retain $M=76$ or 84 states. At the VBS point the infinite-lattice algorithm without the iteration cycles provided almost the same accuracy.

In the extrapolation procedure the $N\to\infty$ limit of the gap was determined by fitting a form $\Delta E(N)=\Delta+a/N$ or $\Delta E(N)=\Delta+b/N^2$ to the energy differences measured between the energy levels of the various S_T sectors. In principle the first has to be used when the gap vanishes, $\Delta=0$, while the second gives the correct asymptotic behavior when the gap is finite.[34] When the gap is finite but the chain length is not long enough to observe the correct parabolic behavior, the linear fit gives a lower-bound estimate.[35] We have used the parabolic fit whenever deviation from the linear dependence on $1/N$ was observed.

IV. NUMERICAL RESULTS

In this section we present our numerical results for the low-lying levels of the model for various choices of the couplings. For a finite ladder the ground state is always a spin singlet. Above this level there are two low-lying triplet excitations, which at $\lambda_1=\lambda_2=\lambda_3=0$ have equal energy. At this point, they correspond to independent excitations on the two decoupled legs. These levels are followed by several $S_T=0,1,2,\ldots,$ excitations. The energy differences between all these levels scale as $1/N$, indicating a gapless excitation spectrum.

For finite values of λ_1,λ_2, and λ_3 the degeneracy of the two low-lying triplet levels is in general lifted. This is shown along the λ_1 axis in Fig. 2. In a finite chain with N sites the energy difference between the lowest triplet and the ground-state singlet levels will be denoted by $\Delta E_{10}(N)$. When this quantity scales to a finite value, the ground state is a nondegenerate singlet with a finite gap. When, however, it scales to zero, we have to consider the next level. This is either the second triplet or it may have been crossed by the lowest $S_T=2$ level. The energy difference between this quintuplet and the ground-state singlet levels will be denoted by $\Delta E_{20}(N)$, while $\Delta E_{21}(N)$ denotes the energy difference between this quintuplet and the lowest triplet levels.

A. Gap opening due to $\mathcal{H}_1$

Let us consider first the effect of $\mathcal{H}_1$, since earlier calculations[18] by exact diagonalization on relatively short chains could not determine satisfactorily the way the gap is opened. For $\lambda_1>0$ the energy of the lowest triplet states and that of the singlet ground state come exponentially close to each other and become degenerate in the thermodynamic limit ($N\to\infty$). This gives the well-known fourfold degeneracy of the VBS-like state in a finite chain with OBC.

Therefore the relevant energy gap can be obtained most easily by measuring the energy difference $\Delta E_{21}(N)$ between the lowest-lying levels of the $S_T=2$ and $S_T=1$ sectors. This energy difference as a function of λ_1 is shown in Fig. 3 for $\lambda_1>0$. The lines connecting the values calculated at several distinct points are only guides to the eye. The inset in the figure shows in more detail the behavior of the gap close to the integrable point.

In the extrapolation to $N\to\infty$ a $1/N$ fit was applied close to the critical point, because the chain lengths were not long enough to observe the parabolic behavior. As an indication of the accuracy of our calculation we mention that at $\lambda_1=1$, where the Haldane gap should be recovered, we obtained $\Delta_{21}=0.41(1)$, in reasonable agreement to three decimal places with its best estimate.[34,36] The ground-state energy divided by the chain length converges to $E_0/N=1.401\,484(0)$, in agreement to six decimal places with earlier calculations.[36]

As a further check we have also performed calculations for large values of λ_1 and used the self-duality relationship in Eq. (9) to obtain the gap for weak couplings. The results obtained in this way are shown in the inset. From this we could also conclude that our finite-size calculations are correct to at least four decimal places. Even though the accuracy of our calculations is limited, we have found a linearly opening energy gap for $\lambda_1>0$. This is the first calculation where this could be demonstrated numerically.

For negative values of λ_1 the coupling between the chains is ferromagnetic, while the ''on-chain'' coupling remains antiferromagnetic. The low-lying part of the spectrum is essentially different from that of the $\lambda_1>0$ regime. The degeneracy of the two $S_T=1$ triplet levels is again lifted, but even the lowest of them will remain separated from the singlet ground state. So the energy difference to be studied is $\Delta E_{10}(N)$. This quantity is shown on the left-hand side of Fig. 3 for $\lambda_1<0$. As can be seen, the ground state is a nondegenerate singlet with a small, but finite gap to the lowest-lying excitations.

Since the gap is small, the value of Δ_{10} has been calculated using the finite-lattice method. This procedure with three iteration cycles and a $1/N$ fit gave at $\lambda_1=-1$, e.g., $\Delta_{10}=0.11(4)$ as a lower-bound estimate for the singlet-triplet gap. Furthermore, the lowest quintuplet level has been found to become degenerate with the lowest triplet state in the thermodynamic limit. Thus a gap separates the ground state from the continuum of excitations.

For small values of λ_1 the accuracy of the calculations has been checked using the relationship in Eq. (10). The gap is found to open linearly. Thus $\mathcal{H}_1$ is relevant for both signs of λ_1.

On the other hand, for large negative values, in the region $\lambda_1<-10$, we have found the vanishing of both Δ_{10} and Δ_{20}. This indicates that a new phase with a gapless spectrum may appear there. However, due to the smallness of the gap around $\lambda_1=-1$, we were unable to locate the point where the transition occurs.

B. Effect of $\mathcal{H}_2$ and $\mathcal{H}_3$

The effect of the interleg coupling $\mathcal{H}_2$ on the decoupled chains described by $\mathcal{H}_0$ for $\lambda_1=\lambda_3=0$ has been considered by several authors.[5,8,10] Hida[5] found that the gap is finite for $\lambda_2<\lambda_{2c}=-0.6$, while Dagotto *et al.*[7] showed some evidence that the critical coupling is closer to zero, perhaps $\lambda_{2c}\approx-0.4$. On the other hand, Watanabe *et al.*[8] and Hsu and Anglès d'Auriac[10] argued that the interchain coupling defined by $\mathcal{H}_2$ is always relevant and $\lambda_{2c}=0$.

We repeated some of these calculations to confirm that this coupling is in fact relevant for both signs of the coupling λ_2. For $\lambda_2>0$ the ground state is a nondegenerate singlet even in the thermodynamic limit with a rather large gap. At $\lambda_2=4/3$, e.g., a singlet-triplet gap with $\Delta_{10}=0.72(9)$, and a singlet-quintuplet gap with $\Delta_{20}=1.43(4)$ has been found.

For $\lambda_2<0$ the spectrum is similar to that for $\lambda_1>0$, where the ground state becomes fourfold-degenerate in the thermodynamic limit. The gap, however, is rather small. At $\lambda_2=-4/3$ the calculation with the finite-lattice method and a $1/N$ fit gave $\Delta_{21}=0.11(3)$, in agreement with previous results.[8]

The plaquette coupling $\mathcal{H}_3$ also turned out to be relevant for both signs of the coupling, but in some sense its effect is opposite to that of $\mathcal{H}_2$. A fourfold, degenerate ground state is obtained with a finite quintuplet-singlet gap for $\lambda_3>0$. At $\lambda_3=4/3$, e.g., $\Delta_{20}=0.28(5)$ has been found. For $\lambda_3<0$ the ground state remains singlet. At $\lambda_3=-4/3$ the triplet-singlet gap is $\Delta_{10}=0.26(8)$.

Because of this opposing effect of these couplings, next we considered the competition of $\mathcal{H}_2$ and $\mathcal{H}_3$ by choosing $\lambda_2=\lambda_3$. For negative values of λ_2 the low-lying part of the energy spectrum resembles very much that found above for small negative λ_1. A finite gap develops between the singlet and triplet levels as shown in Fig. 4. At $\lambda_2=-4/3$ the finite-lattice algorithm and a $1/N$ fit gave $\Delta_{10}=0.17(5)$. Close to the critical point the extrapolated lower-bound values of the gap are even smaller; therefore the available chain lengths are still not long enough to determine the character of the opening of the gap.

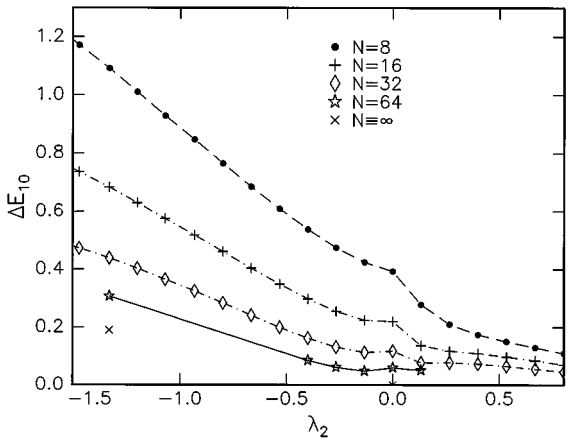

FIG. 4. The energy difference ΔE_{10} as a function of λ_2 at $\lambda_1=\lambda_3=0$. The symbol $\times$ shows the extrapolated value of the gap for $\lambda_2=-4/3$.

On the other hand, for $\lambda_2=\lambda_3>0$ the analysis of the low-lying energy spectrum has shown that both Δ_{10} and Δ_{20} scale to zero; i.e., the spectrum is gapless. Since the system remains critical in an extended region for $\lambda_2=\lambda_3>0$, a Kosterlitz-Thouless-like transition may occur at $\lambda_1=\lambda_2=\lambda_3=0$ to the massive phase at $\lambda_2=\lambda_3<0$. This could explain the slow opening of the gap in that region.

These results are only partially consistent with the field theoretical prediction, which states that the spin-1/2 integrable point is unstable against all perturbations. Our calculations indicate that although both $\mathcal{H}_2$ and $\mathcal{H}_3$ are relevant operators in the ladder model for both signs of the couplings λ_2 and λ_3, the model remains critical at least along the $\lambda_2=\lambda_3>0$ half line.

To summarize our findings, three types of the spectrum have been found. An asymptotically fourfold-degenerate ground state, charateristic of a VBS-like state, is obtained for $\lambda_1>0$, $\lambda_2=\lambda_3=0$, for $\lambda_2<0$, $\lambda_1=\lambda_3=0$, and for $\lambda_3>0$, $\lambda_1=\lambda_2=0$. A truly nondegenerate singlet ground state is found for $\lambda_1<0$, $\lambda_2=\lambda_3=0$, for $\lambda_2>0$, $\lambda_1=\lambda_3=0$, for $\lambda_3<0$, $\lambda_1=\lambda_2=0$, and also for $\lambda_2=\lambda_3<0$, $\lambda_1=0$. Finally the spectrum is gapless for $\lambda_2=\lambda_3>0$, $\lambda_1=0$.

C. Competition of $\mathcal{H}_1$, $\mathcal{H}_2$, and $\mathcal{H}_3$

After having determined the spectrum along the λ_i axes and the $\lambda_2=\lambda_3$ line, next we consider the phase diagram in the parameter space spanned by λ_i. To simplify the calculations we restrict ourselves in the remaining part of the paper to a two-parameter plane by choosing $\lambda_2=\lambda_3$. We will study especially the neighborhood of the $\lambda_1=1$ line, which corresponds to the bilinear-biquadratic Hamiltonian.

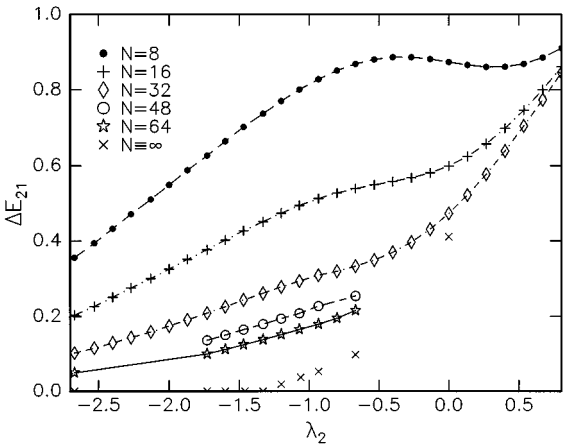

FIG. 5. The quintuplet-triplet energy difference $\Delta E_{21}(N)$ as a function of $\lambda_2=\lambda_3$ at $\lambda_1=1$. Close to the critical point the size of the symbol for the extrapolated gap indicates the error.

In the Takhtajan-Babujian point of the bilinear-biquadratic model, which corresponds to $\lambda_1=1$, $\lambda_2=\lambda_3=-4/3$ in our model, the spectrum is gapless in the thermodynamic limit. Both the singlet-triplet $[\Delta E_{10}(N)]$ and the triplet-quintuplet $[\Delta E_{21}(N)]$ energy differences vanish as $1/N$. They behave, however, quite differently as we move away from the critical point. This is shown in Figs. 5 and 6.

For $\lambda_2>-4/3$ the lowest triplet level becomes asymptotically degenerate with the ground-state singlet, and so the relevant gap is between the triplet and quintuplet levels (Δ_{21}). This level structure is the same as along the $\lambda_1>0$ line; thus a VBS-like state is obtained in this part of the phase space. The opening of the gap is very slow; even our longest chains are too short to obtain a reliable estimate of the gap close to the critical point. The error of the extrapolated value close to the critical point is indicated in Fig. 5 by the size of the symbol.

For $\lambda_2<-4/3$ a finite gap develops between the ground-state singlet and the lowest triplet levels, in the same way as for $\lambda_2=\lambda_3<0$. A lower-bound estimate of the gap obtained by a $1/N$ fit is shown in Fig. 6. The results are in agreement with a linearly opening extrapolated gap Δ_{10}.

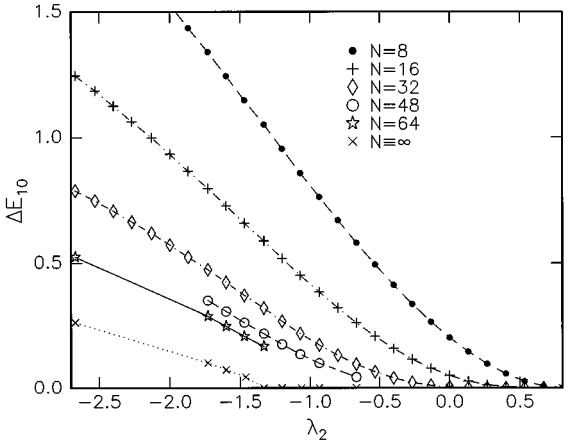

FIG. 6. The same as Fig. 5 for the triplet-singlet energy difference $\Delta E_{10}(N)$.

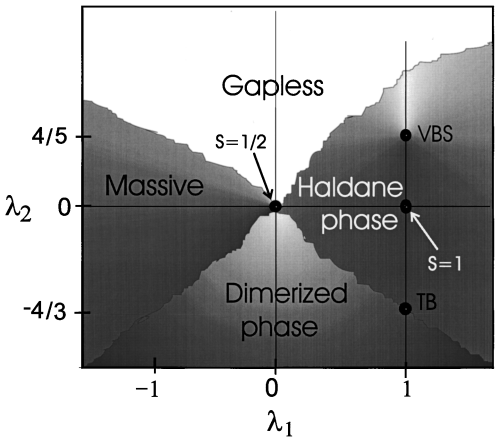

FIG. 7. Schematic phase diagram of the model in the $(\lambda_1,\lambda_2=\lambda_3)$ plane. The wavy lines between the four different phases indicate that the location of the phase boundaries has not been determined accurately.

It is known, however, that the $\lambda_2<-4/3$ region corresponds to a dimerized phase, where instead of a singlet ground state, a doubly degenerate ground state would have to be found. Therefore, we have considered several higher-lying levels to search for the other singlet level that would become degenerate with the ground state. We have not found any such level. This can be understood by recalling that in the case of OPB the dimerized phase gives a truly twofold degenerate ground state only if the number of sites is odd, i.e., if the number of bonds is even. For chains with an even number of sites the energy of the dimerized state depends on whether the bonds at the ends are strong or weak. Inspection of the low-lying levels is therefore not sufficient to distinguish a real nondegenerate singlet ground state from a dimerized state. We will return to this problem later, when the dimer order parameter will be discussed.

One of the two kinds of behavior found for $\lambda_2=\lambda_3>-4/3$ and $\lambda_2=\lambda_3<-4/3$ appears whenever one moves away from the Takhtajan-Babujian integrable point in any direction in the $(\lambda_1,\lambda_2=\lambda_3)$ plane. Varying, e.g., λ_1 around $\lambda_1=1$ at $\lambda_2=\lambda_3=-4/3$, a nondegenerate singlet ground state is found for $\lambda_1<1$, while for $\lambda_1>1$ the singlet-triplet gap disappears, forming a fourfold-degenerate ground state. This result is in agreement with the assumption that the Takhtajan-Babujian point is generically unstable against perturbations, except along the phase boundaries.

Our calculation is, however, not accurate enough to locate this critical line in the phase space that separates the two kinds of behavior. In the schematic phase diagram shown in Fig. 7 the boundaries are therefore indicated by wavy lines. That the phase boundary between the VBS-like Haldane phase and the supposedly dimerized phase connects the $\lambda_1=\lambda_2=\lambda_3=0$ and the Takhtajan-Babujian points has been confirmed by looking at the energy spectrum of our model along the trajectory parametrized by $\lambda_1=1-\lambda$, $\lambda_2=\lambda_3=-4\lambda/3$, where λ varies between 0 and 1. For small values of λ a fourfold-degenerate ground state is recovered, while for λ close to unity a nondegenerate singlet ground state is found.

As mentioned before, this singlet ground state was found along the $\lambda_1<0$, $\lambda_2=\lambda_3=0$ line as well. Whether this axis

also belongs to the dimerized phase or not cannot be determined from the low-lying spectrum alone. We will return to this problem later.

Extending the calculations to $\lambda_2=\lambda_3>0$ on the line $\lambda_1=1$ the VBS-like state survives in a finite range, including the point $\lambda_2=\lambda_3=4/5$, where the exact nearest-neighbor valence bond state is recovered. At this point the lowest singlet and triplet levels are degenerate for any finite chain lengths. The gap reaches its maximum value with $\Delta_{21}=0.8404(7)$, which, after including the appropriate scaling factors due to our normalization to $\lambda_0=1$, agrees to five digits with the known result.[37]

For larger values of λ_2 along the $\lambda_1=1$ line the Lai-Sutherland model and the trimerized phase of the bilinear-biquadratic model cannot be reached by this ladder model. The extra levels introduced by the composite-spin representation will be low lying and will lead to a gapless new phase, as has already been found for $\lambda_1=0$. This massless phase has been found for large positive $\lambda_2=\lambda_3$ values also for $\lambda_1<0$. Thus it is stable in an extended range of the couplings.

D. Dimer order

Even though the structure of the low-lying part of the energy spectrum indicates the existence of various phases, its knowledge, as discussed above, is not sufficient to clarify unambiguously the character of the ground state. We have, therefore, calculated several quantities in the ground state, like the local magnetization $\langle\vec{S}_i\rangle\equiv\langle\vec{\sigma}_i\rangle+\langle\vec{\tau}_i\rangle$, the two-point correlation function $\langle\vec{S}_i\vec{S}_j\rangle\equiv\langle(\vec{\sigma}_i+\vec{\tau}_i)(\vec{\sigma}_j+\vec{\tau}_j)\rangle$, and the local energy $E_{\rm loc}\equiv\langle\mathcal{H}(i,i+1)\rangle$, where $\mathcal{H}(i,i+1)$ contains the couplings between spins on sites i and $i+1$.

The correlation function falls off exponentially both in the Haldane and the dimerized phases, turning to power law like on the phase boundary, but the chains are still too short to distinguish clearly between these two possibilities. A better procedure could be to look at the local magnetization in the lowest triplet state. Due to the free end spins of the exact nearest-neighbor valence-bond configuration, the local magnetization is finite close to the chain ends in the VBS-like Haldane phase. Approaching the phase boundary, the extra spin becomes less and less localized and it spreads out homogeneously in the dimerized and gapless phases.

The most useful procedure is, however, to consider the so-called short-range dimer order parameter. It can be defined by taking the difference of the local energy on neighboring bonds in the middle of the ladder,

$$R_{\rm srdo}=\frac{\langle\mathcal{H}(i,i+1)\rangle-\langle\mathcal{H}(i+1,i+2)\rangle}{\frac{1}{2}\left[\langle\mathcal{H}(i,i+1)\rangle+\langle\mathcal{H}(i+1,i+2)\rangle\right]}. \qquad (11)$$

It is expected to have different behavior if the ground state is unique, fourfold degenerate, or twofold degenerate as in the dimerized state with spontaneously broken translational symmetry.

A simpler quantity can be defined by taking the bilinear part of the coupling only:

$$S_{\rm srdo}=\frac{\langle\vec{S}_i\cdot\vec{S}_{i+1}\rangle-\langle\vec{S}_{i+1}\cdot\vec{S}_{i+2}\rangle}{\frac{1}{2}\left[\langle\vec{S}_i\cdot\vec{S}_{i+1}\rangle+\langle\vec{S}_{i+1}\cdot\vec{S}_{i+2}\rangle\right]}. \qquad (12)$$

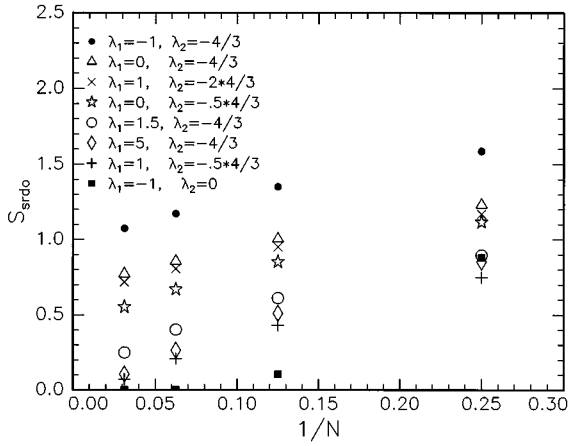

FIG. 8. The short-range dimer order parameter $S_{\rm srdo}$ calculated in the middle of the chain vs the inverse of the chain length at a few points of the phase space $(\lambda_1,\lambda_2=\lambda_3)$.

In Fig. 8 we present our results for the short-range dimer order parameter $S_{\rm srdo}$ measured in the middle of the ladder as a function of the inverse of the chain length for a few points of the $(\lambda_1,\lambda_2=\lambda_3)$ phase space. The parameter $R_{\rm srdo}$ not shown in the figure gives the same kind of behavior.

There is clearly an extended region in the parameter space, where the short-range order parameter scales to zero in the thermodynamic limit. At the VBS point itself $S_{\rm srdo}$ was found to be zero for short finite chains already. The vanishing of $S_{\rm srdo}$ happens not only in the Haldane phase, but also along the negative λ_1 axis and in a neighborhood of it, where the spectrum was indistinguishable from the spectrum of the supposedly dimerized state.

For large negative values of λ_2, however, both for positive and negative values of λ_1, a transition was found to the state where $R_{\rm srdo}$ and $S_{\rm srdo}$ have nonzero values and the local magnetization at the ends of the chain vanishes. Thus, in the region where the ground state was found to be a nondegenerate singlet, the short-range dimer order allows us to distinguish two regimes. In the region denoted as ''dimerized phase'' in Fig. 7, both $R_{\rm srdo}$ and $S_{\rm srdo}$ scale to a finite value. In this phase the local magnetization at the ends of the chain is also absent. In the other region marked as ''massive,'' the dimer order disappears. The boundary between them is drawn schematically only in Fig. 7, and its exact shape could not be determined, except that it has to go through the $\lambda_1=\lambda_2=\lambda_3=0$ point.

V. CONCLUSIONS

In the present paper we have considered a two-leg ladder model constructed from a composite-spin model. Besides the usual Heisenberg coupling between the spins on the legs interleg coupling between spins on the same and neighboring rungs have been introduced, as well as four-spin plaquette couplings.

For special values of these couplings this ladder model is equivalent to the spin-1/2 Heisenberg model or the spin-1 bilinear-biquadratic model in the sense that the low-lying parts of the spectra are identical. Thus massless, VBS-like, and dimerized phases are expected to appear, but the phase diagram can be even richer.

The behavior of the energy differences between low-lying levels has been calculated using the DMRG method and the gap extrapolated to the thermodynamic limit ($N\to\infty$) was obtained with the method of finite-size scaling. We have also considered the short-range dimer order parameter.

It has been found that the spin-1/2 Heisenberg ladder is unstable against most of the perturbations that couple the two legs, but there is a small range of the parameters where the combination of the perturbing operators is irrelevant.

Four different kinds of behavior was observed, as shown in Fig. 7. In a region along and near to the line $\lambda_1=0$, $\lambda_2=\lambda_3>0$ the spectrum remains gapless. Everywhere else a gap is developed in the spectrum. Three regions can, however, be distinguished depending on whether the ground state is nondegenerate or twofold or fourfold degenerate. The last case is easily detected by studying the asymptotic degeneracy of the spectrum. This phase is present around the $\lambda_1=1$, $\lambda_2=\lambda_3=4/5$ point, where the exact nearest-neighbor valence-bond state is recovered. The extra $s=1/2$ spins at the ends of the chains become more and more delocalized as we move away from the VBS point and disappear at the phase boundary, where the transition is either to the gapless phase or to a dimerized one.

The Takhtajan-Babujian point at $\lambda_1=1$, $\lambda_2=\lambda_3=-4/3$ lies on the phase boundary between the VBS-like and the dimerized phases. The transition here could be detected not only in the change of the character of the spectrum, but also by the appearance of a finite short-range dimer order parameter. This quantity was used to distinguish the dimer phase also from the ''massive'' phase with a nondegenerate singlet ground state, where the dimer order disappears again, in fact much faster than $1/N$.

Unfortunately, our limited computational resources did not allow us to determine the precise location of the critical lines separating the various phases.

ACKNOWLEDGMENTS

This research was supported in part by the Hungarian Research Fund (OTKA) Grant No. 15870, by the Swiss National Science Foundation Grant No. 20-37642.93, the ISI Foundation (Torino), and the EU PECO Network ERBCIPDCT940027.

*On leave from the Research Institute for Solid State Physics, Budapest, Hungary.

[1] D. C. Johnston, J. W. Johnson, D. P. Goshorn, and A. J. Jacobson, Phys. Rev. B **35**, 219 (1987).
[2] Z. Hiroi, M. Azuma, M. Takano, and Y. Bando, J. Solid State Chem. **95**, 230 (1991).
[3] R. J. Cava *et al.*, J. Solid State Chem. **94**, 170 (1991).
[4] F. D. M. Haldane, Phys. Rev. Lett. **50**, 1153 (1983); Phys. Lett. **93A**, 464 (1983).
[5] K. Hida, J. Phys. Soc. Jpn. **60**, 1347 (1991); **60**, 1939 (1991).
[6] S. P. Strong and A. J. Millis, Phys. Rev. Lett. **69**, 2419 (1992).
[7] E. Dagotto, J. Riera, and D. Scalapino, Phys. Rev. B **45**, 5744 (1992).
[8] S. Takada and H. Watanabe, J. Phys. Soc. Jpn. **61**, 39 (1992); H. Watanabe, K. Nomura, and S. Takada, *ibid*. **62**, 2845 (1993); H. Watanabe, Phys. Rev. B **50**, 13 442 (1994).
[9] T. Barnes, E. Dagotto, J. Riera, and E. S. Swanson, Phys. Rev. B **47**, 3196 (1993); T. Barnes and J. Riera, *ibid*. **50**, 6817 (1994).
[10] T. Hsu and J. C. Anglès d'Auriac, Phys. Rev. B **47**, 14 291 (1993).
[11] R. M. Noack, S. R. White, and D. J. Scalapino, Phys. Rev. Lett. **73**, 882 (1994); S. R. White, R. M. Noack, and D. J. Scalapino, *ibid*. **73**, 886 (1994).
[12] S. Gopalan, T. M. Rice, and M. Sigrist, Phys. Rev. B **49**, 8901 (1994); M. Sigrist, T. M. Rice, and F. C. Zhang, *ibid*. **49**, 12 058 (1994).
[13] H. Tsunetsugu, M. Troyer, and T. M. Rice, Phys. Rev. B **49**, 16 078 (1994); M. Troyer, H. Tsunetsugu, and D. Würtz, *ibid*. **50**, 13 515 (1994).
[14] K. Totsuka and M. Suzuki, J. Phys. Condens. Matter **7**, 6079 (1995).
[15] S. R. White, Phys. Rev. B **53**, 52 (1996).
[16] R. S. Eccleston, T. Barnes, J. Brody, and J. W. Johnson, Phys. Rev. Lett. **73**, 2626 (1994).
[17] M. Azuma, Z. Hiroi, M. Takano, K. Ishida, and Y. Kitaoka, Phys. Rev. Lett. **73**, 3463 (1994).
[18] J. Sólyom and J. Timonen, Phys. Rev. B **34**, 487 (1986); **38**, 6832 (1988); **39**, 7003 (1989).
[19] H. J. Schulz, Phys. Rev. B **34**, 6372 (1986).
[20] S. R. White, Phys. Rev. Lett. **69**, 2863 (1992); Phys. Rev. B **48**, 10 345 (1993).
[21] I. Affleck, Phys. Rev. Lett. **55**, 1355 (1985); Nucl. Phys. **B265**, 409 (1986).
[22] L. Takhtajan, Phys. Lett. **87A**, 479 (1982); H. M. Babujian, *ibid*. **90A**, 479 (1982).
[23] C. K. Lai, J. Math. Phys. **15**, 1675 (1974); B. Sutherland, Phys. Rev. B **12**, 3795 (1975).
[24] I. Affleck, T. Kennedy, E. H. Lieb, and H. Tasaki, Phys. Rev. Lett. **59**, 799 (1987); Commun. Math. Phys. **115**, 477 (1988).
[25] J. B. Parkinson, J. Phys. C **21**, 3793 (1988); M. N. Barber and M. T. Bachelor, Phys. Rev. B **40**, 4621 (1989); A. Klümper, J. Phys. A **23**, 809 (1990).
[26] D. Kung (unpublished); J. Oitmaa, J. B. Parkinson, and J. C. Bonner, J. Phys. C **19**, L595 (1986); H. W. J. Blöte and H. W. Capel, Physica **139A**, 387 (1986).
[27] J. Sólyom, Phys. Rev. B **36**, 8642 (1987).
[28] K. Nomura and S. Takada, J. Phys. Soc. Jpn. **60**, 389 (1991).
[29] G. Fáth and J. Sólyom, Phys. Rev. B **44**, 11 836 (1991); **47**, 872 (1993).
[30] C. Itoi and M. H. Kato (unpublished).
[31] A. V. Chubukov, Phys. Rev. B **43**, 3337 (1991).
[32] G. Fáth and J. Sólyom, Phys. Rev. B **51**, 3620 (1995).
[33] Ö. Legeza and G. Fáth, Phys. Rev. B **53**, 14 349 (1996).
[34] E. S. Sorensen and I. Affleck, Phys. Rev. Lett. **71**, 1633 (1993).
[35] U. Schollwöck and T. Jolicoeur, Europhys. Lett. **30**, 493 (1995).
[36] S. R. White and D. A. Huse, Phys. Rev. B **48**, 3844 (1993).
[37] G. Fáth and J. Sólyom, J. Phys. Condens. Matter **5**, 8983 (1993).